verified, immunoreactivity of antibody against sugar chain of α-DG is decreased in these diseases [42, 43], supporting the idea that it is a glycosyltransferase.

Muscle-eye-brain (MEB) disease, found mainly in Finland, is characterized by severe brain and ocular abnormalities as well as congenital muscular dystrophy. Interestingly, mutations of the *POMGnT1* gene were identified in patients with MEB [44]. POMGnT1 was shown to catalyze the GlcNAcβ1-2Man linkage in the O-mannosyl glycan of α-DG and *in vitro* experiment demonstrated that the enzyme activity is lost by introducing the mutations found in the patients [44,45]. Walker-Warburg syndrome (WWS) is one of the most severe types of CMD accompanied by brain malformation and structural eye abnormalities. The brains of WWS patients are more severely affected than those of FCMD or MEB. O-mannosyltransferase 1 (POMT1) and O-mannosyltransferase 2 (POMT2) are involved in O-mannosylation of glycoproteins, the first step in which mannose is attached to serine or threonine residues. These are very unique enzyme, *i.e.*, either POMT1 or POMT2 alone dose not exhibit any glycosyltransferase activity [46]. To exert their function as O-mannosyltransferase, they need to form a complex [47]. First, point mutations were found in the *POMT1* gene then in the *POMT2* gene in WWS patients [48, 49]. However, mutation of POMT1 and POMT2 accounts only less than one-third of the whole WWS patients and further responsible genes are to be elucidated.

Mutations of a putative glycosyltransferase, large, were first identified in mouse models of muscular dystrophy, Large$^{myd}$, Large$^{vls}$ and *enr* mouse [50, 51]. A point mutation of Large was also identified in a patient with CMD accompanied by brain malformation. α-DG in the skeletal muscle of this patient is aberrantly glycosylated and this disease is classified as congenital muscular dystrophy 1D (MDC1D) [52]. Large is localized to Golgi apparatus and composed of tandem putative catalytic domain of glycosyltransferase, however its enzymatic activity has not been demonstrated yet. The features of each α-dystroglycanopathy are summarized in table 1.

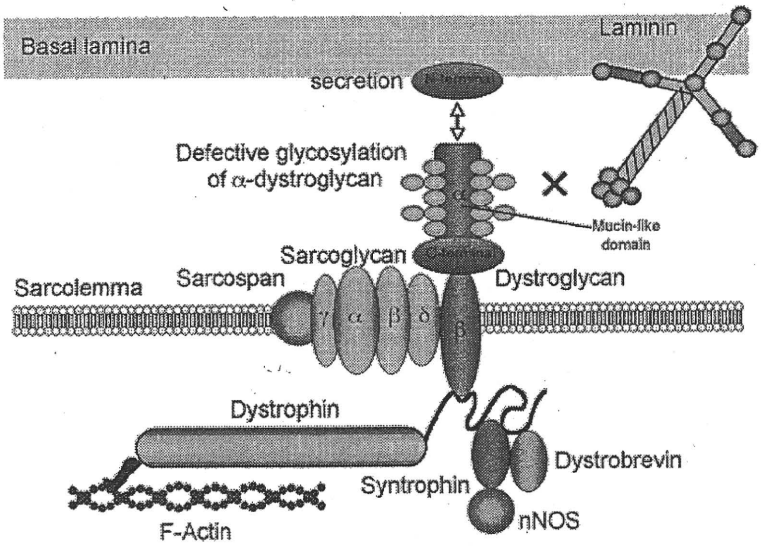


Figure 2. Disruption of dystroglycan-laminin linkage in α-dystroglycanopathy.
In α-dystroglycanopathy, the glycosylation of α-dystroglycan (α-DG) is defective due to the mutations of known or putative glycosyltransferases. This results in the loss of α-DG binding to laminin, therefore, the axis connecting cytoskeleton and extracellular matrix is disrupted.

**Table 1. Summary of α-dystroglycanopathy and clinical symptoms. -, not involved; +, mildly involved; ++, moderately involved; +++, severely involved.**

| | | | Clinical symptom | | |
|---|---|---|---|---|---|
| Disease | Abbreviation | Gene product | Muscle | Brain | Eye |
| CMD with secondary merosin deficiency 2 | ÇlDC1C | FKRP | ++ | - | - |
| Limb-girdle muscular dystrophy type 2I | LGMD2I | FKRP | + | - | - |
| CMD with mental retardation and pachygyria | MDC1D | Large | ++ | + | - |
| Fukuyama type CMD | FCMD | Fukutin | ++ | ++ | ++ |
| Muscle-eye-brain disease | MEB | POMGnT1 | ++ | ++ | ++ |
| Walker-Warburg syndrome | WWS | POMT1, POMT2 | +++ | +++ | +++ |

Michele et al. convincingly demonstrated using antibody against core protein of α-DG that in the skeletal muscle of α-dystroglycanopathy patients, α-DG is hypoglycosylated due to the mutations of glycosyltransferases and the binding activity of this α-DG molecule to its ligands such as laminin, agrin and neurexin is severely reduced (Figure 2) [53]. These findings are consistent with previous reports describing that the sugar chain moiety of α-DG, especially O-mannosyl glycan, is crucial for the α-DG-laminin interaction [22]. Disruption of the linkage between α-DG and laminin should have profound effects on the muscle cells viability because it causes destabilization of the sarcolemma against contraction-stretch stress, hampers signal transduction and inhibits assembly of ECM proteins [17]. Interestingly, Barresi et al. reported that overexpression of Large facilitates the glycosylation of α-DG and restores the ligand binding activity of α-DG in myoblasts from patients of α-dystroglycanopathy such as FCMD or MEB disease [54]. In addition, it was shown that partial restoration of α-DG glycosylation and laminin binding activity is sufficient to maintain skeletal muscle function [55]. Therefore, modulation of the expression of Large could provide a novel therapeutic strategy for α-dystroglycanopathy in the future.

## DYSFUNCTION OF DG AND MOLECULAR BASIS OF BRAIN ANOMALY

One of the prominent hallmarks of α-dystroglycanopathy is the presence of the brain anomaly. The brain anomaly observed in α-dystroglycanopathy patients includes micropolygyria, disarray of cerebral cortical layering, interhemispheric fusion, abnormal cerebellar foliation, hydrocephalus, glioneuronal heterotopia in subarachnoid space and these anomalies are collectively termed lissencephaly type 2 or cobblestone lissencephaly [56]. Similar brain malformation has been described in Large$^{myd}$ mice [57]. It is of particular importance to note that glia limitans-basal lamina is frequently disrupted and neuroglial tissues protrude through the cleft into the subarachnoid space in FCMD brains [58]. This disruption of the glia limitans-basal lamina causes migration defects of neuron and eventually results in the anomaly such as disarray of cerebral cortical layering or formation of the peculiar appearance of the micropolygyria in this disorder.

Similar to skeletal muscle, the hypoglycosylation and reduced laminin binding activity of α-DG were demonstrated in Large$^{myd}$ mouse brain [53]. Because a constitutive disruption of dystroglycan results in embryonic lethality of mouse [6], Moore et al. utilized Cre-loxP system and disrupted the dystroglycan gene selectively in brain [59]. Because DG mainly localizes to the foot-process of astrocyte that constitutes glia limitans at the pial surface, they used GFAP promoter to drive the expression of cre-recombinase in astrocyte. Surprisingly, this mouse exhibited extremely similar neuropathological findings to those of FCMD, MEB, WWS and Large$^{myd}$ mouse [59]. Furthermore, it was demonstrated that laminin binding activity is lost in the brain and glia limitans-basal lamina was severely disrupted in the brain of this mouse [59]. Recently, the same brain malformation, including disrupted glia limitans-basal lamina, was demonstrated in mice with specific loss of α-DG in epiblast. In these mice, the laminin binding activity of α-DG was severely reduced in brain [60]. These observations strongly support the idea that the functional defect in α-DG is central to the pathogenesis of brain malformation in CMD. Interestingly, DG is also expressed by oligodendrocytes and plays a role, by interacting with laminin, in regulating terminal stages of myelination, such as myelin membrane production, growth, or stability in central nervous system [61].

It should also be noted that dystroglycan is expressed in neurons in addition to glial cells in several locations including hippocampus [62, 63]. Because cre-recombinase is transiently expressed in neuronal progenitor cells in the GFAP-DG null mouse, dystroglycan is ablated also in neurons in the mouse. Interestingly, it was shown that hippocampal long-term potentiation is blunted possibly by a postsynaptic mechanism in the GFAP-DG null mouse [59]. These results raise an intriguing possibility that neuronal dystroglycan is playing an important role in learning and memory and the mental retardation seen in FCMD, MEB and WWS patients may be in part attributed to the dysfunction of the neuronal dystroglycan. It has been reported that DG localizes inhibitory synapses and α-DG binds to neurexin [12], whereas β-DG interacts with synaptic scaffolding molecule (S-SCAM) [64].

## VERSATILE FUNCTION OF DG IN PERIPHERAL NERVE

In peripheral nerve, DG is localized to outer membrane of Schwann cells and binds to laminin 2 in the endoneurial basal lamina [65]. Mutation of laminin α2 chain results in congenital muscular dystrophy type 1A (MDC1A). It is known that in MDC1A patients as well as in its rodent model, dy/dy mouse, dysmyelination of peripheral nerve develops in addition to muscular dystrophy. Myelinating Schwann cells express dystroglycan and integrin (α6β1 and α6β4) as laminin receptors [66]. Recently, conditional knockout mouse of β1 integrin in peripheral nerve revealed that β1 integrin is essential for the radial sorting of axon, a process in which a Schwann cell wraps a single axon with 1:1 relationship [67]. DG is another candidate for a laminin 2 receptor involved in myelination, because it is co-expressed with laminin 2 during peripheral nerve myelination and regeneration after nerve crush injury [68]. Therefore, it has been speculated that the α-DG-laminin interaction is necessary for the myelin formation and its maintenance in peripheral nerve.

To test this hypothesis, we have generated mice deficient in DG selectively in Schwann cells by crossing DG floxed mice with P0 promoter driven cre-recombinase expressing transgenic mice [69]. Interestingly, the peripheral nerves of this mouse exhibited broad

spectrum of morphological abnormalities. Myelin sheath was extensively folded, which is consisted of multiple external myelin loops. Polyaxonal myelination, in which single myelin sheath wraps multiple axons, and single Schwann cells including multiple myelinated axons were observed. The latter finding indicates that radial sorting mechanism is disturbed in this mouse [69]. In addition to these myelination defects, formation of the node of Ranvier was abnormal. Microvillis in node, where DG localizes, was disorganized and blunted in this mouse. In consistent to this structural defect, clustering of $Na^+$ channel was strikingly reduced at the node of Ranvier [69]. Recently, we also observed defective myelination of peripheral nerve in fukutin deficient chimeric mouse, a model mouse of FCMD. In this mouse, myelinated fiber density is decreased and numerous clusters of non-myelinated fibers, which indicate defective radial sorting, are observed [70]. Interestingly, neuromuscular junction is fragmented in appearance and clustering of acetylcholine receptor is defective in this mouse [70]. The laminin binding activity of α-DG is severely decreased in the skeletal muscle as well as neuromuscular junction, indicating that the α-DG-laminin interaction is crucial for normal myelin sheath and neuromuscular junction formation and/or their maintenance.

Apart from the extracellular linkage of DG, cytoplasmic linkage is also associated to dysmyelination of peripheral nerve. Cytoplasmic domain of β-DG binds dystrophin related protein 2 (DRP2), and DRP2 in turn interact with L-periaxin in Schwann cells [71]. It has been reported that L-periaxin deficient mice exhibit peripheral neuropathy [72]. Consistent with this observation, mutations in L-periaxin gene were identified in patients with hereditary peripheral neuropathy, Charcot-Marie-Tooth disease type 4F and Dejerine-Sottas disease [73, 74]. Taken together, disruption of both the extracellular and intracellular linkage mediated by DG leads to impaired myelin formation in peripheral nerve.

DG is a target of infectious diseases. *Mycobacterium leprae* (*M. leprae*), the causative organism of leprosy, a pathogen that preferentially infects Schwann cells. The LG like domain of laminin α2 chain is an initial target of *M. leprae* and they attach to the domain via 21kD laminin binding protein and phenolic glycolipid 1, molecules in the bacterial cell wall [75]. Then, α-DG on the plasma membrane of Schwann cells serves as a receptor for *M. leprae* to invade in Schwann cells [76]. Interestingly, it was shown that *M. leprae* cause demyelination by a contact depending mechanism in the absence of immune cells [77]. Lymphocytic choriomeningitis virus (LCMV) and several other arenaviruses including Lassa fever virus also utilize α-DG as a receptor [78]. Large dependent O-mannosyl glycosylation of α-DG is crucial for the virus-host interaction [79, 80]. Interestingly, infection of arenavirus to Schwann cell perturbates laminin-α-DG linkage, resulting in myelination defect in peripheral nerve [81].

## CONCLUSION

A broad spectrum of neuromuscular diseases is now attributed to dysfunction of dystroglycan. Especially, recent progress in molecular genetics and biochemistry in this area revealed that defective glycosylation of α-DG underlies the pathogenesis of muscular dystrophy. The defective glycosylation results in both degeneration of the skeletal muscle and migration defects of neuron in the brain via disruption of DG-laminin linkage. Apart from these tissues, defective DG function also affects myelination and radial sorting of the

peripheral nerve. Both the extracellular interaction through α-DG-laminin and the intracellular interaction through β-DG-DRP2-L-periaxin are essential for these basic biological processes in peripheral nerve. Intact DG function is also necessary for the formation of neuromuscular junction and the clustering of $Na^+$ channel at the node of Ranvier. When we seek therapeutic procedures for this wide variety of neuromuscular disorders, amelioration or up-regulation of DG function could be a most suitable molecular target. In this regard, putative glycosyltransferase Large is now known to restore the defective DG function, thus it is an intriguing idea to apply this effect of Large to the therapy for α-dystroglycanopathy. Further experiments are necessary to shed further lights on the pathomechanism and to facilitate the development of therapeutic strategy for these disorders.

## ACKNOWLEDGEMENTS

We thank Miki Ikeda for her expert technical assistance. This work was supported by [1] Research Grants 16B-1, 17A-10, 19A-5 and 20B-13 for Nervous and Mental Disorders, Research on Psychiatric and Neurological Diseases and Mental Health H20-016 (Ministry of Health, Labor and Welfare), [2] Research Grant 16390256, 40286993, 17590898, 19591010 and "Open Research Center" Project for Private Universities: matching fund subsidy from MEXT (Ministry of Education, Culture, Sports, Science and Technology), 2004-2008.

## REFERENCES

[1] Ervasti, J. M. & Campbell, K. P. (1991). Membrane organization of the dystrophin-glycoprotein complex. *Cell, 66*, 1121-31.

[2] Brenman, J. E., Chao, D. S., Gee, S. H., McGee, A. W., Craven, S. E., Santillano, D. R., Wu, Z., Huang, F., Xia, H., Peters, M. F., Froehner, S. C. & Bredt, D. (1996). Interaction of nitric oxide synthase with the postsynaptic density protein PSD-95 and α1-syntrophin mediated by PDZ domains. *Cell, 84*, 757-67.

[3] Ayalon, G., Davis, J. Q., Scotland, P. B. & Bennett, V. (2008). An ankyrin-based mechanism for functional organization of dystrophin and dystroglycan. *Cell, 135*, 1189-200.

[4] Straub, V. & Campbell, K. P. (1997). Muscular dystrophies and the dystrophin-glycoprotein complex. *Curr Opin Neurol., 10*, 168-75.

[5] Helbling-Leclerc, A., Zhang, X., Topaloglu, H., Cruaud, C., Tesson, F., Weissenbach, J., Tomé, F. M., Schwartz, K., Fardeau, M., Tryggvason, K. & Guicheney, P. (1995). Mutations in the laminin α2-chain gene (LAMA2) cause merosin-deficient congenital muscular dystrophy. *Nat Genet., 11*, 216-8.

[6] Williamson, R. A., Henry, M. D., Daniels, K. J., Hrstka, R. F., Lee, J. C., Sunada, Y., Ibraghimov-Beskrovnaya, O. & Campbell, K. P. (1997). Dystroglycan is essential for early embryonic development: disruption of Reichert's membrane in Dag1-null mice. *Hum Mol Genet., 6*, 831-41.

[7] Ibraghimov-Beskrovnaya, O., Ervasti, J. M., Leveille, C. J., Slaughter, C. A., Sernett, S. W. & Campbell, K. P. (1992). Primary structure of dystrophin-associated glycoproteins linking dystrophin to the extracellular matrix. *Nature, 355*, 696-702.

[8] Akhavan, A., Crivelli, S. N., Singh, M., Lingappa, V. R. & Muschler, J. L. (2008). SEA domain proteolysis determines the functional composition of dystroglycan. *FASEB J., 22*, 612-21.

[9] Ervasti, J. M. & Campbell, K. P. (1993). A role for the dystrophin-glycoprotein complex as a transmembrane linker between laminin and actin. *J Cell Biol., 122*, 809-23.

[10] Bowe, M. A., Deyst, K. A., Leszyk, J. D. & Fallon, J. R. (1994). Identification and purification of an agrin receptor from Torpedo postsynaptic membranes: a heteromeric complex related to the dystroglycans. *Neuron., 12*, 1173-80.

[11] Peng, H. B., Ali, A. A., Daggett, D. F., Rauvala, H., Hassell, J. R. & Smalheiser, N. R. (1998). The relationship between perlecan and dystroglycan and its implication in the formation of the neuromuscular junction. *Cell Adhes Commun., 5*, 475-89.

[12] Sugita, S., Saito, F., Tang, J., Satz, J., Campbell, K. & Südhof, T. C. (2001). A stoichiometric complex of neurexins and dystroglycan in brain. *J Cell Biol., 154*, 435-45.

[13] Sato, S., Omori, Y., Katoh, K., Kondo, M., Kanagawa, M., Miyata, K., Funabiki, K., Koyasu, T., Kajimura, N., Miyoshim, T., Sawai, H., Kobayashi, K., Tani, A., Toda, T., Usukura, J., Tano, Y., Fujikado, T. & Furukawa, T. (2008). Pikachurin, a dystroglycan ligand, is essential for photoreceptor ribbon synapse formation. *Nat Neurosci., 11*, 923-31.

[14] Bowe, M. A., Mendis, D. B. & Fallon, J. R. (2000). The small leucine-rich repeat proteoglycan biglycan binds to α-dystroglycan and is upregulated in dystrophic muscle. *J Cell Biol., 148*, 801-10.

[15] Suzuki, A., Yoshida, M., Hayashi, K., Mizuno, Y., Hagiwara, Y. & Ozawa, E. (1994). Molecular organization at the glycoprotein-complex-binding site of dystrophin. Three dystrophin-associated proteins bind directly to the carboxy-terminal portion of dystrophin. *Eur J Biochem., 220*, 283-92.

[16] Durbeej, M., Larsson, E., Ibraghimov-Beskrovnaya, O., Roberds, S. L., Campbell, K. P. & Ekblom, P. (1995). Non-muscle α-dystroglycan is involved in epithelial development. *J Cell Biol., 130*, 79-91.

[17] Henry, M. D. & Campbell, K. P. (1998). A role for dystroglycan in basement membrane assembly. *Cell, 95*, 859-70.

[18] Kanagawa, M., Saito, F., Kunz, S., Yoshida-Moriguchi, T., Barresi, R., Kobayashi, Y. M., Muschler, J., Dumanski, J. P., Michele, D. E., Oldstone, M. B. & Campbell, K. P. (2004). Molecular recognition by LARGE is essential for expression of functional dystroglycan. *Cell, 117*, 953-64.

[19] Singh, J., Itahana, Y., Knight-Krajewski, S., Kanagawa, M., Campbell, K. P., Bissell, M. J. & Muschler, J. (2004). Proteolytic enzymes and altered glycosylation modulate dystroglycan function in carcinoma cells. *Cancer Res., 64*, 6152-9.

[20] Saito, F., Saito-Arai, Y., Nakamura, A., Shimizu, T. & Matsumura, K. (2008). Processing and secretion of the N-terminal domain of α-dystroglycan in cell culture media. *FEBS Lett., 582*, 439-44.

[21] Sciandra, F., Schneider, M., Giardina, B., Baumgartner, S., Petrucci, T. C. & Brancaccio, A. (2001). Identification of the β-dystroglycan binding epitope within the C-terminal region of α-dystroglycan. *Eur J Biochem.*, *268*, 4590-7.

[22] Chiba, A., Matsumura, K., Yamada, H., Inazu, T., Shimizu, T., Kusunoki, S., Kanazawa, I., Kobata, A. & Endo, T. (1997). Structures of sialylated O-linked oligosaccharides of bovine peripheral nerve α-dystroglycan. The role of a novel O-mannosyl-type oligosaccharide in the binding of α-dystroglycan with laminin. *J Biol Chem.*, *272*, 2156-62.

[23] Endo, T. (1999). O-mannosyl glycans in mammals. *Biochim Biophys Acta.*, *1473*, 237-46.

[24] Manya, H., Suzuki, T., Akasaka-Manya, K., Ishida, H. K., Mizuno, M., Suzuki, Y., Inazu, T., Dohmae, N. & Endo, T. (2007). Regulation of mammalian protein O-mannosylation: preferential amino acid sequence for O-mannose modification. *J Biol Chem.*, *282*, 20200-6.

[25] Yang, B., Jung, D., Motto, D., Meyer, J., Koretzky, G. & Campbell, K. P. (1995). SH3 domain-mediated interaction of dystroglycan and Grb2. *J Biol Chem.*, *270*, 11711-4.

[26] James, M., Nuttall, A., Ilsley, J. L., Ottersbach, K., Tinsley, J. M., Sudol, M. & Winder, S. J. (2000). Adhesion-dependent tyrosine phosphorylation of β-dystroglycan regulates its interaction with utrophin. *J Cell Sci.*, *113*, 1717-26.

[27] Ilsley, J. L., Sudol, M. & Winder, S. J. (2001). The interaction of dystrophin with β-dystroglycan is regulated by tyrosine phosphorylation. *Cell Signal.*, *13*, 625-32.

[28] Sotgia, F., Lee, H., Bedford, M. T., Petrucci, T., Sudol, M. & Lisanti, M. P. (2001). Tyrosine phosphorylation of β-dystroglycan at its WW domain binding motif, PPxY, recruits SH2 domain containing proteins. *Biochemistry*, *40*, 14585-92.

[29] Langenbach, K. J. & Rando, T. A. (2002). Inhibition of dystroglycan binding to laminin disrupts the PI3K/AKT pathway and survival signaling in muscle cells. *Muscle Nerve.*, *26*, 644-53.

[30] Spence, H. J., Chen, Y. J., Batchelor, C. L., Higginson, J. R., Suila, H., Carpen, O. & Winder, S. J. (2004). Ezrin-dependent regulation of the actin cytoskeleton by β-dystroglycan. *Hum Mol Genet.*, *13*, 1657-68.

[31] Zhou, Y., Jiang, D., Thomason, D. B. & Jarrett, H. W. (2007). Laminin-induced activation of Rac1 and JNKp46 is initiated by Src family kinases and mimics the effects of skeletal muscle contraction. *Biochemistry*, *46*, 14907-16.

[32] Boffi, A., Bozzi, M., Sciandra, F., Woellner, C., Bigotti, M. G., Ilari, A. & Brancaccio, A. (2001). Plasticity of secondary structure in the N-terminal region of β-dystroglycan. *Biochim Biophys Acta.*, *1546*, 114-21.

[33] Yamada, H., Saito, F., Fukuta-Ohi, H., Zhong, D., Hase, A., Arai, K., Okuyama, A., Maekawa, R., Shimizu, T. & Matsumura, K. (2001). Processing of β-dystroglycan by matrix metalloproteinase disrupts the link between the extracellular matrix and cell membrane via the dystroglycan complex. *Hum Mol Genet.*, *10*, 1563-9.

[34] Zhong, D., Saito, F., Saito, Y., Nakamura, A., Shimizu, T. & Matsumura, K. (2006). Characterization of the protease activity that cleaves the extracellular domain of β-dystroglycan. *Biochem Biophys Res Commun.*, *345*, 867-71.

[35] Matsumura, K., Arai, K., Zhong, D., Saito, F., Fukuta-Ohi, H., Maekawa, R., Yamada, H. & Shimizu, T. (2003). Disruption of dystroglycan axis by β-dystroglycan processing in cardiomyopathic hamster muscle. *Neuromuscul Disord.*, *13*, 796-803.

[36] Matsumura, K., Zhong, D., Saito, F., Arai, K., Adachi, K., Kawai, H., Higuchi, I., Nishino, I. & Shimizu, T. (2005). Proteolysis of β-dystroglycan in muscular diseases. *Neuromuscul Disord.*, *15*, 336-41.

[37] Michaluk, P., Kolodziej, L., Mioduszewska, B., Wilczynski, G. M., Dzwonek, J., Jaworski, J., Gorecki, D. C., Ottersen, O. P. & Kaczmarek, L. (2007). β-dystroglycan as a target for MMP-9, in response to enhanced neuronal activity. *J Biol Chem.*, *282*, 16036-41.

[38] Toda, T., Kobayashi, K., Takeda, S., Sasaki, J., Kurahashi, H., Kano, H., Tachikawa, M., Wang, F., Nagai, Y., Taniguchi, K., Taniguchi, M., Sunada, Y., Terashima, T., Endo, T. & Matsumura, K. (2003). Fukuyama-type congenital muscular dystrophy (FCMD) and α-dystroglycanopathy. *Congenit Anom (Kyoto)*, *43*, 97-104.

[39] Kobayashi, K., Nakahori, Y., Miyake, M., Matsumura, K., Kondo-Iida, E., Nomura, Y., Segawa, M., Yoshioka, M., Saito, K., Osawa, M., Hamano, K., Sakakihara, Y., Nonaka, I., Nakagome, Y., Kanazawa, I., Nakamura, Y., Tokunaga, K. & Toda, T. (1998). An ancient retrotransposal insertion causes Fukuyama-type congenital muscular dystrophy. *Nature*, *394*, 388-92.

[40] Hayashi, Y. K., Ogawa, M., Tagawa, K., Noguchi, S., Ishihara, T., Nonaka, I. & Arahata, K. (2001). Selective deficiency of α-dystroglycan in Fukuyama-type congenital muscular dystrophy. *Neurology*, *57*, 115-21.

[41] Xiong, H., Kobayashi, K., Tachikawa, M., Manya, H., Takeda, S., Chiyonobu, T., Fujikake, N., Wang, F., Nishimoto, A., Morris, G. E., Nagai, Y., Kanagawa, M., Endo, T. & Toda, T. (2006). Molecular interaction between fukutin and POMGnT1 in the glycosylation pathway of α-dystroglycan. *Biochem Biophys Res Commun.*, *350*, 935-41.

[42] Brockington, M., Blake, D. J., Prandini, P., Brown, S. C., Torelli, S., Benson, M. A., Ponting, C. P., Estournet, B., Romero, N. B., Mercuri, E., Voit, T., Sewry, C. A., Guicheney, P. & Muntoni, F. (2001). Mutations in the fukutin-related protein gene (FKRP) cause a form of congenital muscular dystrophy with secondary laminin α2 deficiency and abnormal glycosylation of α-dystroglycan. *Am J Hum Genet.*, *69*, 1198-209.

[43] Brockington, M., Yuva, Y., Prandini, P., Brown, S. C., Torelli, S., Benson, M. A., Herrmann, R., Anderson, L. V., Bashir, R., Burgunder, J. M., Fallet, S., Romero, N., Fardeau, M., Straub, V., Storey, G., Pollitt, C., Richard, I., Sewry, C. A., Bushby, K., Voit, T., Blake, D. J. & Muntoni, F. (2001). Mutations in the fukutin-related protein gene (FKRP) identify limb girdle muscular dystrophy 2I as a milder allelic variant of congenital muscular dystrophy MDC1C. *Hum Mol Genet.*, *10*, 2851-9.

[44] Yoshida, A., Kobayashi, K., Manya, H., Taniguchi, K., Kano, H., Mizuno, M., Inazu, T., Mitsuhashi, H., Takahashi, S., Takeuchi, M., Herrmann, R., Straub, V., Talim, B., Voit, T., Topaloglu, H., Toda, T. & Endo, T. (2001). Muscular dystrophy and neuronal migration disorder caused by mutations in a glycosyltransferase, POMGnT1. *Dev Cell*, *1*, 717-24.

[45] Kano, H., Kobayashi, K., Herrmann, R., Tachikawa, M., Manya, H., Nishino, I., Nonaka, I., Straub, V., Talim, B., Voit, T., Topaloglu, H., Endo, T., Yoshikawa, H. &

Toda, T. (2002). Deficiency of α-dystroglycan in muscle-eye-brain disease. *Biochem Biophys Res Commun.*, *291*, 1283-6.

[46] Manya, H., Chiba, A., Yoshida, A., Wang, X., Chiba, Y., Jigami, Y., Margolis, R. U. & Endo, T. (2004). Demonstration of mammalian protein O-mannosyltransferase activity: coexpression of POMT1 and POMT2 required for enzymatic activity. *Proc Natl Acad Sci.*, U. S. A., *101*, 500-5.

[47] Akasaka-Manya, K., Manya, H., Nakajima, A., Kawakita, M. & Endo, T. (2006). Physical and functional association of human protein O-mannosyltransferases 1 and 2. *J Biol Chem.*, *281*, 19339-45.

[48] Beltrán-Valero de Bernabé, D., Currier, S., Steinbrecher, A., Celli, J., van Beusekom, E., van der Zwaag, B., Kayserili, H., Merlini, L., Chitayat, D., Dobyns, W. B., Cormand, B., Lehesjoki, A. E., Cruces, J., Voit, T., Walsh, C. A., van Bokhoven, H. & Brunner, H. G. (2002). Mutations in the O-mannosyltransferase gene POMT1 give rise to the severe neuronal migration disorder Walker-Warburg syndrome. *Am J Hum Genet.*, *71*, 1033-43.

[49] van Reeuwijk, J., Janssen, M., van den Elzen, C., Beltran-Valero de Bernabé, D., Sabatelli, P., Merlini, L., Boon, M., Scheffer, H., Brockington, M., Muntoni, F., Huynen, M. A., Verrips, A., Walsh, C. A., Barth, P. G., Brunner, H. G. & van Bokhoven, H. (2005). POMT2 mutations cause α-dystroglycan hypoglycosylation and Walker-Warburg syndrome. *J Med Genet.*, *42*, 907-12.

[50] Grewal, P. K., Holzfeind, P. J., Bittner, R. E. & Hewitt, J. E. (2001). Mutant glycosyltransferase and altered glycosylation of α-dystroglycan in the myodystrophy mouse. *Nat Genet.*, *28*, 151-4.

[51] Lee, Y., Kameya, S., Cox, G. A., Hsu, J., Hicks, W., Maddatu, T. P., Smith, R. S., Naggert, J. K., Peachey, N. S. & Nishina, P. M. (2005). Ocular abnormalities in Large (myd) and Large(vls) mice, spontaneous models for muscle, eye, and brain diseases. *Mol Cell Neurosci.*, *30*, 160-72.

[52] Longman, C., Brockington, M., Torelli, S., Jimenez-Mallebrera, C., Kennedy, C., Khalil, N., Feng, L., Saran, R. K., Voit, T., Merlini, L., Sewry, C. A., Brown, S. C., Muntoni, F. (2003). Mutations in the human LARGE gene cause MDC1D, a novel form of congenital muscular dystrophy with severe mental retardation and abnormal glycosylation of α-dystroglycan. *Hum Mol Genet.*, *12*, 2853-61.

[53] Michele, D. E., Barresi, R., Kanagawa, M., Saito, F., Cohn, R. D., Satz, J. S., Dollar, J., Nishino, I., Kelley, R. I., Somer, H., Straub, V., Mathews, K. D., Moore, S. A. & Campbell, K. P. (2002). Post-translational disruption of dystroglycan-ligand interactions in congenital muscular dystrophies. *Nature*, *418*, 417-22.

[54] Barresi, R., Michele, D. E., Kanagawa, M., Harper, H. A., Dovico, S. A., Satz, J. S., Moore, S. A., Zhang, W., Schachter, H., Dumanski, J. P., Cohn, R. D., Nishino, I. & Campbell, K. P. (2004). LARGE can functionally bypass α-dystroglycan glycosylation defects in distinct congenital muscular dystrophies. *Nat Med.*, *10*, 696-703.

[55] Kanagawa, M., Nishimoto, A., Chiyonobu, T., Takeda, S., Miyagoe-Suzuki, Y., Wang, F., Fujikake, N., Taniguchi, M., Lu, Z., Tachikawa, M., Nagai, Y., Tashiro, F., Miyazaki, J., Tajima, Y., Takeda, S., Endo, T., Kobayashi, K., Campbell, K. P., Toda, T. (2009). Residual laminin-binding activity and enhanced dystroglycan glycosylation by LARGE in novel model mice to dystroglycanopathy. *Hum Mol Genet.*, *18*, 621-31.

[56] Ross, M. E. & Walsh, C. A. (2001). Human brain malformations and their lessons for neuronal migration. *Annu Rev Neurosci., 24*, 1041-70.

[57] Holzfeind, P. J., Grewal, P. K., Reitsamer, H. A., Kechvar, J., Lassmann, H., Hoeger, H., Hewitt, J. E. & Bittner, R. E. (2002). Skeletal, cardiac and tongue muscle pathology, defective retinal transmission, and neuronal migration defects in the Large(myd) mouse defines a natural model for glycosylation-deficient muscle - eye - brain disorders. *Hum Mol Genet., 11*, 2673-87.

[58] Saito, Y., Murayama, S., Kawai, M. & Nakano, I. (1999). Breached cerebral glia limitans-basal lamina complex in Fukuyama-type congenital muscular dystrophy. *Acta Neuropathol, 98*, 330-6.

[59] Moore, S. A., Saito, F., Chen, J., Michele, D. E., Henry, M. D., Messing, A., Cohn, R. D., Ross-Barta, S. E., Westra, S., Williamson, R. A., Hoshi, T. & Campbell, K. P. (2002). Deletion of brain dystroglycan recapitulates aspects of congenital muscular dystrophy. *Nature, 418*, 422-5.

[60] Satz, J. S., Barresi, R., Durbeej, M., Willer, T., Turner, A., Moore, S. A. & Campbell, K. P. (2008). Brain and eye malformations resembling Walker-Warburg syndrome are recapitulated in mice by dystroglycan deletion in the epiblast. *J Neurosci., 28*, 10567-75.

[61] Colognato, H., Galvin, J., Wang, Z., Relucio, J., Nguyen, T., Harrison, D., Yurchenco, P. D. & Ffrench-Constant, C. (2007). Identification of dystroglycan as a second laminin receptor in oligodendrocytes, with a role in myelination. *Development, 134*, 1723-36.

[62] Górecki, D. C., Derry, J. M. & Barnard, E. A. (1994). Dystroglycan: brain localisation and chromosome mapping in the mouse. *Hum Mol Genet.*, 3, 1589-97.

[63] Zaccaria, M. L., Di Tommaso, F., Brancaccio, A., Paggi, P. & Petrucci, T. C. (2001). Dystroglycan distribution in adult mouse brain: a light and electron microscopy study. *Neuroscience, 104*, 311-24.

[64] Sumita, K., Sato, Y., Iida, J., Kawata, A., Hamano, M., Hirabayashi, S., Ohno, K., Peles, E. & Hata, Y. (2007). Synaptic scaffolding molecule (S-SCAM) membrane-associated guanylate kinase with inverted organization (MAGI)-2 is associated with cell adhesion molecules at inhibitory synapses in rat hippocampal neurons. *J Neurochem., 100*, 154-66.

[65] Yamada, H., Shimizu, T., Tanaka, T., Campbell, K. P. & Matsumura, K. (1994). Dystroglycan is a binding protein of laminin and merosin in peripheral nerve. *FEBS Lett., 352*, 49-53.

[66] Previtali, S. C., Feltri, M. L., Archelos, J. J., Quattrini, A., Wrabetz, L. & Hartung, H. (2001). Role of integrins in the peripheral nervous system. *Prog Neurobiol., 64*, 35-49.

[67] Feltri, M. L., Graus Porta, D., Previtali, S. C., Nodari, A., Migliavacca, B., Cassetti, A., Littlewood-Evans, A., Reichardt, L. F., Messing, A., Quattrini, A., Mueller, U. & Wrabetz, L. (2002). Conditional disruption of beta 1 integrin in Schwann cells impedes interactions with axons. *J Cell Biol., 156*, 199-209.

[68] Masaki, T., Matsumura, K., Hirata, A., Yamada, H., Hase, A., Arai, K., Shimizu, T., Yorifuji, H., Motoyoshi, K. & Kamakura, K. (2002). Expression of dystroglycan and the laminin-α 2 chain in the rat peripheral nerve during development. *Exp Neurol., 174*, 109-17.

[69] Saito, F., Moore, S. A., Barresi, R., Henry, M. D., Messing, A., Ross-Barta, S. E., Cohn, R. D., Williamson, R. A., Sluka, K. A., Sherman, D. L., Brophy, P. J., Schmelzer, J. D., Low, P. A., Wrabetz, L., Feltri, M. L. & Campbell, K. P. (2003).

Unique role of dystroglycan in peripheral nerve myelination, nodal structure, and sodium channel stabilization. *Neuron, 38*, 747-58.

[70] Saito, F., Masaki, T., Saito, Y., Nakamura, A., Takeda, S., Shimizu, T., Toda, T. & Matsumura, K. (2007). Defective peripheral nerve myelination and neuromuscular junction formation in fukutin-deficient chimeric mice. *J Neurochem., 101*, 1712-22.

[71] Sherman, D. L., Fabrizi, C., Gillespie, C. S. & Brophy, P. J. (2001). Specific disruption of a schwann cell dystrophin-related protein complex in a demyelinating neuropathy. *Neuron, 30*, 677-87.

[72] Gillespie, C. S., Sherman, D. L., Fleetwood-Walker, S. M., Cottrell, D. F., Tait, S., Garry, E. M. Wallace, V. C., Ure, J., Griffiths, I. R., Smith, A. & Brophy, P. J. (2000). Peripheral demyelination and neuropathic pain behavior in periaxin-deficient mice. *Neuron, 26*, 523-31.

[73] Boerkoel, C. F., Takashima, H., Stankiewicz, P., Garcia, C. A., Leber, S. M., Rhee-Morris, L. & Lupski, J. R. (2001). Periaxin mutations cause recessive Dejerine-Sottas neuropathy. *Am J Hum Genet., 68*, 325-33.

[74] Guilbot, A., Williams, A., Ravisé, N., Verny, C., Brice, A., Sherman, D. L., Brophy, P. J., LeGuern, E., Delague, V., Bareil, C., Mégarbané, A. & Claustres, M. (2001). A mutation in periaxin is responsible for CMT4F, an autosomal recessive form of Charcot-Marie-Tooth disease. *Hum Mol Genet., 10*, 415-21.

[75] Ng, V., Zanazzi, G., Timpl, R., Talts, J. F., Salzer, J. L. & Brennan, P. J. (2000). Rambukkana, A., Role of the cell wall phenolic glycolipid-1 in the peripheral nerve predilection of Mycobacterium leprae. *Cell, 103*, 511-24.

[76] Rambukkana, A., Yamada, H., Zanazzi, G., Mathus, T., Salzer, J. L., Yurchenco, P. D., Campbell, K. P. & Fischetti, V. A. (1998). Role of α-dystroglycan as a Schwann cell receptor for Mycobacterium leprae. *Science, 282*, 2076-9.

[77] Rambukkana, A., Zanazzi, G., Tapinos, N. & Salzer, J. L. (2002). Contact-dependent demyelination by Mycobacterium leprae in the absence of immune cells. *Science, 296*, 927-31.

[78] Cao, W., Henry, M. D., Borrow, P., Yamada, H., Elder, J. H., Ravkov, E. V., Nichol, S. T., Compans, R. W., Campbell, K. P. & Oldstone, M. B. (1998). Identification of α-dystroglycan as a receptor for lymphocytic choriomeningitis virus and Lassa fever virus. *Science, 282*, 2079-81.

[79] Kunz, S., Rojek, J. M., Kanagawa, M., Spiropoulou, C. F., Barresi, R., Campbell, K. P. & Oldstone, M. B. (2005). Posttranslational modification of α-dystroglycan, the cellular receptor for arenaviruses, by the glycosyltransferase LARGE is critical for virus binding. *J Virol., 79*, 14282-96.

[80] Imperiali, M., Thoma, C., Pavoni, E., Brancaccio, A., Callewaert, N. & Oxenius, A. (2005). O Mannosylation of α-dystroglycan is essential for lymphocytic choriomeningitis virus receptor function. *J Virol., 79*, 14297-308.

[81] Rambukkana, A., Kunz, S., Min, J., Campbell, K. P. & Oldstone, M. B. (2003). Targeting Schwann cells by nonlytic arenaviral infection selectively inhibits myelination. *Proc Natl Acad Sci.*, U. S. A., *100*, 16071-6.

Gene Therapy (2008), 1–5

www.nature.com/gt

SHORT COMMUNICATION

# Atelocollagen-mediated local and systemic applications of myostatin-targeting siRNA increase skeletal muscle mass

N Kinouchi[1], Y Ohsawa[2], N Ishimaru[3], H Ohuchi[4], Y Sunada[2], Y Hayashi[3], Y Tanimoto[1], K Moriyama[1,5] and S Noji[4]

[1]Department of Orthodontics and Dentofacial Orthopedics, Graduate School of Dentistry, The University of Tokushima, Tokushima, Japan; [2]Department of Internal Medicine, Division of Neurology, Kawasaki Medical School, Okayama, Japan; [3]Department of Oral Molecular Pathology, Institute of Health Bioscience, The University of Tokushima Graduate School, Tokushima, Japan and [4]Department of Life Systems, Institute of Technology and Science, The University of Tokushima, Tokushima, Japan

*RNA interference (RNAi) offers a novel therapeutic strategy based on the highly specific and efficient silencing of a target gene. Since it relies on small interfering RNAs (siRNAs), a major issue is the delivery of therapeutically active siRNAs into the target tissue/target cells* in vivo. *For safety reasons, strategies based on vector delivery may be of only limited clinical use. The more desirable approach is to directly apply active siRNAs* in vivo. *Here, we report the effectiveness of* in vivo *siRNA delivery into skeletal muscles of normal or diseased mice through nanoparticle formation of chemically unmodified siRNAs with atelocollagen (ATCOL). ATCOL-mediated local application of siRNA targeting myostatin, a negative regulator of skeletal muscle growth, in mouse skeletal muscles or intravenously, caused a marked increase in the muscle mass within a few weeks after application. These results imply that ATCOL-mediated application of siRNAs is a powerful tool for future therapeutic use for diseases including muscular atrophy.*
Gene Therapy advance online publication, 6 March 2008; doi:10.1038/gt.2008.24

**Keywords:** *myostatin; RNA interference; atelocollagen; muscle; mouse; muscular dystrophy*

RNA interference (RNAi) is the process of sequence-specific, posttranscriptional gene silencing in plants and animals from flatworms to human,[1] which is mediated by ~22-nucleotide small interfering RNAs (siRNAs) generated from longer double-stranded RNA. Since it was demonstrated that siRNAs can intervene gene silencing in mammalian cells without induction of interferon synthesis or nonspecific gene suppression,[2] an increasing number of remedies utilizing highly specific siRNAs targeted against disease-causing or disease-promoting genes have been developed.[3] Effective delivery of active siRNAs to target organs or tissues is therefore the key to the development of RNAi as a broad therapeutic platform. For this purpose, different strategies have been used to deliver and achieve RNAi-mediated gene silencing *in vivo*;[3] for example, polymers represent a class of materials that meet the needs of a particular siRNA delivery system, condensing siRNAs into nano-sized particles taken up by cells.[4] However, some of the synthetic polymers, which have been used for delivery of nucleic acids, may trigger cell death in a variety of cell lines and thus suffer from limitations for its application in siRNA delivery *in vivo*.[4] On the other hand, atelocollagen (ATCOL), a pepsin-treated type I collagen lacking in telopeptides in N and C terminals that confer its antigenicity, has been shown to elicit an efficient delivery of chemically unmodified siRNAs to metastatic tumors *in vivo*.[5–7] In this study, we sought to examine the effectiveness of siRNA-ATCOL therapy for a nontumorous systemic disease, targeted against myostatin (growth/differentiation factor 8, GDF8), a negative regulator of skeletal muscle growth.[8]

Skeletal muscles are the crucial morphofunctional organs, and their atrophy causes severe conditions for life such as muscular dystrophies. Duchenne muscular dystrophy (DMD), for instance, is a severe muscle wasting disorder affecting 1 out of 3500 male birth.[9] There is currently no effective treatment, but gene therapy approaches are offering viable avenues for treatment development.[10] As one of therapeutic approaches, inhibition of myostatin by using anti-myostatin-blocking antibodies has been employed to increase muscle mass.[11] However, generating antibodies against recombinant target proteins is time consuming and requires a lot of efforts. Recently, we demonstrated that inhibition of myostatin by overexpression of the myostatin prodomain[12] prevented muscular atrophy and

Correspondence: Professor S Noji or Dr H Ohuchi, Department of Life Systems, Institute of Technology and Science, The University of Tokushima, 2-1 Minami-Jyosanjima-cho, Tokushima 770-8506, Japan.
E-mails: noji@bio.tokushima-u.ac.jp or hohuchi@bio.tokushima-u.ac.jp
[5]Current address: Department of Maxillofacial Orthognathics, Graduate School, Tokyo Medical and Dental University, Tokyo, Japan.
Received 10 October 2007; revised 26 November 2007; accepted 23 January 2008

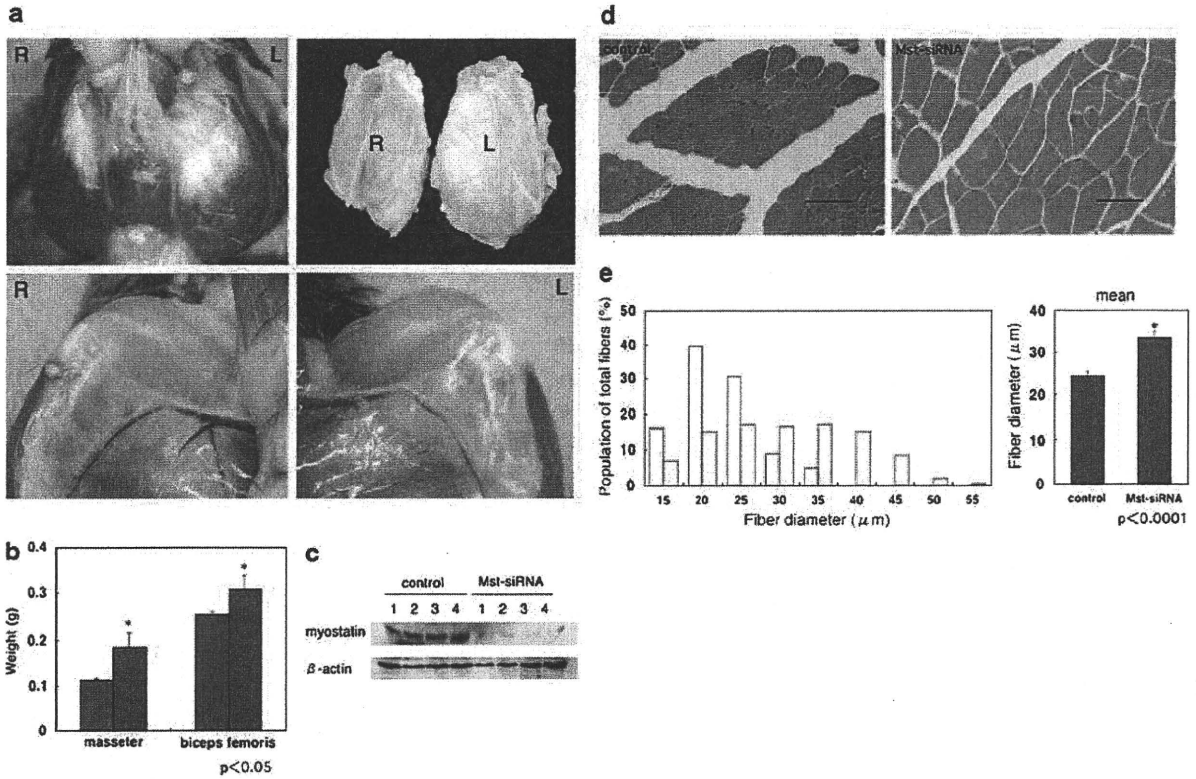


**Figure 1** Local administration of the Mst-siRNA/atelocollagen (ATCOL) complex increases skeletal muscle mass and fiber size in wild-type mice through inhibition of myostatin expression. For the experiments depicted in (**a**–**e**) Mst-siRNAs (final concentration, 10 μM) were mixed with ATCOL (final concentration for local administration, 0.5%.[5]) (AteloGene, Kohken, Tokyo, Japan) according to the manufacturer's instructions. After anesthesia of mice (20-week-old male C57BL/6) by Nembutal (25 mg/kg, i.p.), the Mst-siRNA/ATCOL complex was injected into the masseter and biceps femoris muscles on the left side. As a control, scrambled siRNA/ATCOL complex was injected into the contralateral (right) muscles. After 2 weeks, the muscles on both sides were harvested and processed for analysis. (**a**) Photographs of muscles. Increased muscle mass were observed in the Mst-siRNA/ATCOL-treated (L) masseter (upper panels) and biceps femoris (lower panels), but not in the contralateral muscles (R). (**b**) Muscle weight. Mst-siRNA/ATCOL-treated muscles had an increased weight significantly compared to those with control siRNA/ATCOL (masseter, 0.185 ± 0.041 versus 0.115 ± 0.019 g; biceps, 0.307 ± 0.040 versus 0.232 ± 0.039 g; $n = 4$; $P < 0.05$). Student's *t*-test was used for determining statistical significance. Graphical representation of data uses the following convention: mean ± s.d.; treated muscles or mice in red; control muscles or mice in blue. (**c**) Western blot analysis of myostatin (52 kDa) in the control and Mst-siRNA/ATCOL-treated masseter muscles, assessed at 2 weeks after single injection. Total 80 μg of masseter muscle homogenates were resolved by sodium dodecyl sulfate–polyacrylamide gel electrophoresis and then transferred onto polyvinylidene difluoride membranes for immunoblotting. After a blocking reaction (5% nonfat milk/1% bovine serum albumin in phosphate-buffered saline (PBS) and 0.05% Triton X-100), the blots were incubated for 1 h at room temperature with mouse monoclonal anti-myostatin antibody (1:500; R&D Systems, Minneapolis, MN, USA) or anti-β-actin. After incubation with a secondary antibody (1:10000; horseradish peroxidase-conjugated anti-rat antibody; Biosource International, Camarillo, CA, USA), the blots were developed using the ECL Plus kit (Amersham, Buckinghamshire, UK). We used a purified myostatin protein and proteins extracted from cells transformed with a myostatin cDNA to confirm that the bands are due to 52 kDa myostatin. (**d**) Hematoxylin and eosin staining of the control and Mst-siRNA/ATCOL-treated masseter muscle. Muscles were fixed in 4% paraformaldehyde/PBS at 4 °C overnight, dehydrated and paraffin-embedded. Serial sections (5 μm thickness) were cut at mid-belly of muscle and stained. Scale bar, 50 μm. (**e**) Distribution of myofibril sizes of the control (blue bars) and Mst-siRNA/ATCOL-treated (red bars) muscles. The right panel shows the average myofibril size (33.6 ± 1.5 versus 24.4 ± 1.1 μm; $n = 200$; $P < 0.0001$). NIH Image (NIH, USA) software was used for morphometric measurements.

normalized intracellular myostatin signaling in the model mice for limb-girdle muscular dystrophy 1C.[13] On the other hand, Magee *et al.*[14] demonstrated that downregulation of myostatin expression by transduction of a plasmid expressing a short-hairpin interfering RNA (shRNA) against myostatin using electroporation can increase local skeletal muscle mass. For safety reasons, however, strategies based on vector delivery may be of only limited clinical use. The more desirable approach is to directly apply active siRNAs *in vivo*. As one of the practical platforms for siRNA delivery, we sought to employ an ATCOL-mediated oligonucleotide delivery system to apply myostatin-targeting siRNA into muscles.

We utilized the siRNA sequences reported previously[14] (GDF8 siRNA26, 5′-AAGATGACGATTAT CACGCTA-3′, position 426–446). It has been noted that this sequence can target myostatin mRNA not only of mouse but also human, rat, rabbit, cow, macaque and baboon, based on Blast search (National Center for Biotechnology Information).[14] To confirm the silencing effect of this siRNA, we constructed a plasmid of pSilencer 2.1-U6 neo containing the target sequence and transfected the plasmid into a mouse myoblast cell line, C2C12 cells, which had been made forced to stably express myostatin. We confirmed that the RNAi construct could effectively downregulate the expression

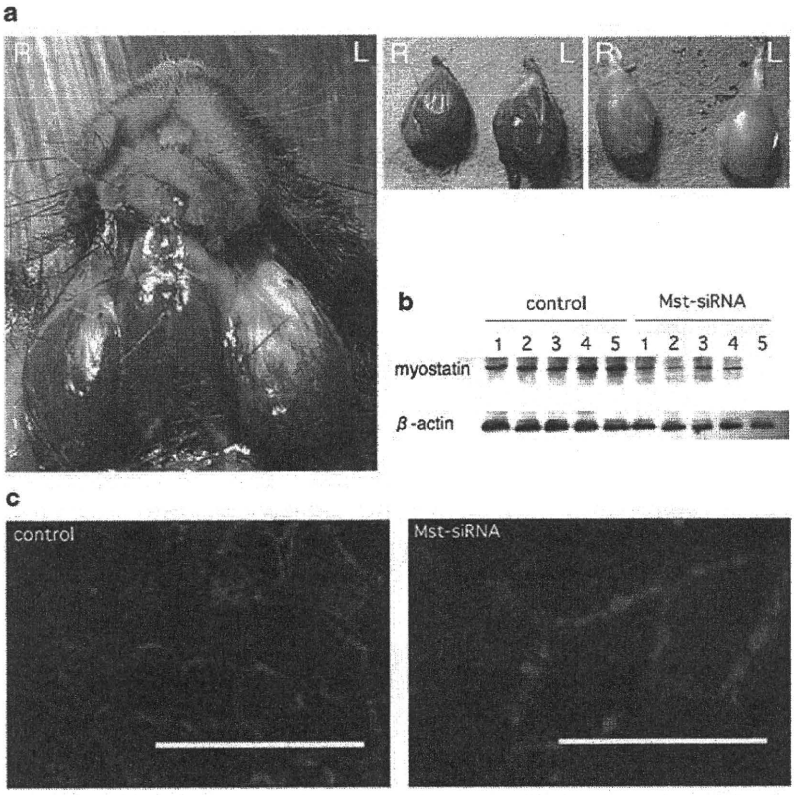


**Figure 2** Mst-siRNA/atelocollagen (ATCOL) treatment improves myofibril size in *mdx* mice. (**a**) Photographs of muscles. The leftward masseter (left and middle panels) and tibial (right panel) muscles injected with the Mst-siRNA/ATCOL complex intramuscularly show a marked increased muscle mass in 20-week-old *mdx* male mice. (**b**) Western blot analysis of the control and Mst-siRNA/ATCOL-treated masseter muscles, assessed at 2 weeks after single injection. Myostatin protein levels in the muscles injected with the Mst-siRNA/ATCOL complex are markedly decreased, but not in the contralateral muscles injected with the control-siRNA/ATCOL. (**c**) Immunohistochemical analysis of the cross-sectional myofiber area of the masseter muscle, with the anti-laminin α2 antibody (4H8-2, Sigma, St Louis, MO, USA), showing increased fiber size in the Mst-siRNA/ATCOL-treated (right panel) muscle, compared to that of control (left panel). Alexafluor 594-conjugated anti-rat immunoglobulin G antibodies (A-11007, Invitrogen, Carlsbad, CA, USA) were used for immunohistochemistry. Scale bar, 100 μm.

of myostatin in the C2C12 cells[15] (Supplementary Figure S1).

We prepared the nanoparticle complex containing the GDF8 siRNA26 (10 μM) and ATCOL. Then, we injected the GDF8 siRNA26-ATCOL (Mst-siRNA/ATCOL) complex into the masseter and biceps femoris muscles of 20-week-old C57BL/6 mice. As a control, we injected control-scrambled siRNAs/ATCOL complex in the contralateral muscles. We observed gross morphology of the muscles and dissected the muscle tissues 2 weeks after injection. After injection of the Mst-siRNA/ATCOL complex, both muscles (on the left side) were enlarged, while no significant change was observed on the contralateral side (Figure 1a). We also measured the muscle weight, finding that the Mst-siRNA/ATCOL-treated muscles weighed significantly more than those on the control side (Figure 1b). The Mst-siRNA/ATCOL-treated muscles were further examined by a western blot analysis for myostatin (52 kDa), showing the decreased expression of myostatin on the treated side (Figure 1c). We quantified each result as a ratio to the internal control and statistically analyzed a difference between control (average ratio $0.90 \pm 0.07$) and treated (average ratio $0.44 \pm 0.22$) muscles. This difference is significant ($P < 0.01$, Student's $t$-test, $n = 4$). Histological analysis showed that the myofibril sizes of the masseter muscles treated with the Mst-siRNA/ATCOL complex were larger than those of the control (Figure 1d). Examining the sizes of 200 myofibers per group, the population of myofibril sizes indicated a shift from smaller to larger fibers in the Mst-siRNA/ATCOL-treated muscle (Figure 1e). The average myofibril size of the muscle treated with Mst-siRNA/ATCOL gained approximately 1.3 times more than that of control (Figure 1e). No obvious morphological change was observed in other tissues than the treated masseter muscles. In the meanwhile, we did not observe any general sign of ill health and deaths during the period of experiment. These results indicate that the increase of the Mst-siRNA/ATCOL-treated muscle mass is caused by their hypertrophy and that the siRNA complex gives no obvious adverse effects.

We next questioned whether this effect of hypertrophy after local injection of the Mst-siRNA/ATCOL complex observed in normal mice was relevant to dystrophin-deficient *mdx* mouse, an animal model for DMD.[16] We intramuscularly injected the same Mst-siRNA/ATCOL complex into the masseter and tibial muscles on the left side of 20-week-old *mdx* male mice. Within 2 weeks after the single injection, a dramatically increased muscle

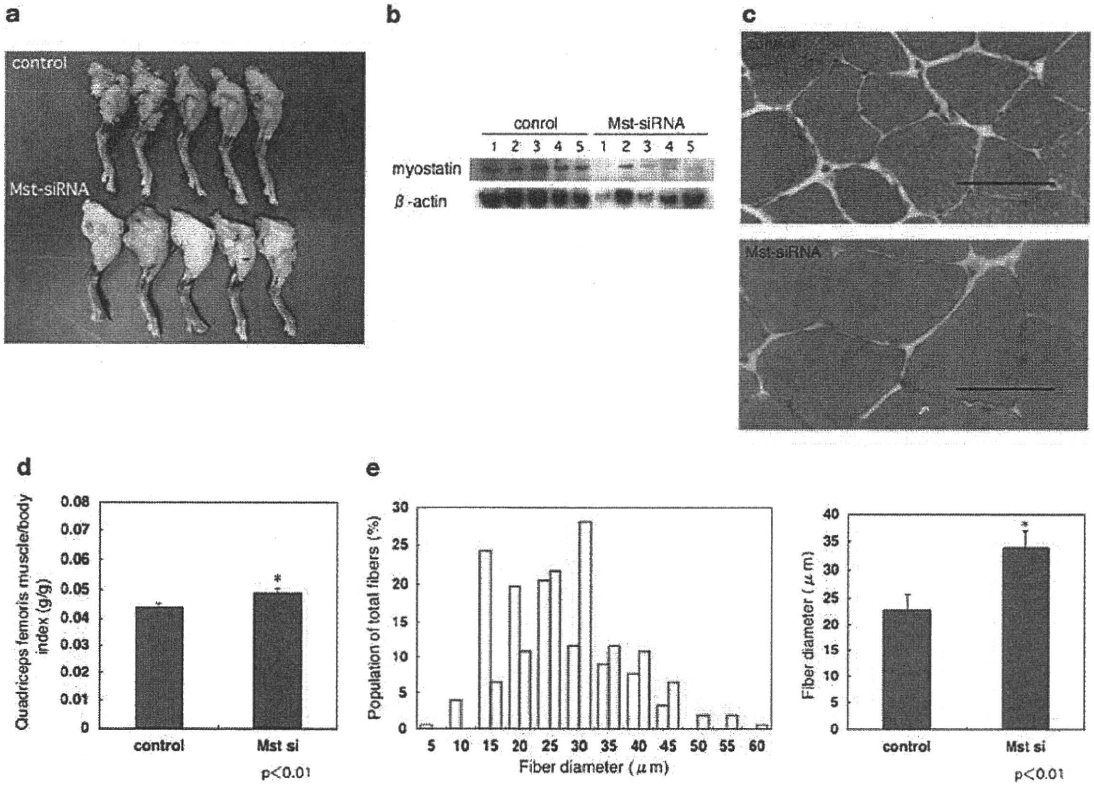


**Figure 3** Systemic administration of the Mst-siRNA/atelocollagen (ATCOL) complex induces muscle enlargement in the mouse through inhibition of myostatin expression. For systemic administration, the siRNA (final concentration, 40 μM)/ATCOL (final concentration, 0.05%[6] complex, 200 μl) was introduced intravenously via orbital veins at 4, 7 and 14 days after the first application ($n=5$). As a control, control-scrambled siRNAs were injected into wild-type male mice (20 weeks, $n=5$). After 3 weeks, the quadriceps muscles on both sides were harvested and processed for analysis. (**a**) Photographs of lower limbs from control (upper panel) and Mst-siRNA/ATCOL-treated (lower panel) mice. (**b**) Western blot analysis of the control and Mst-siRNA/ATCOL-treated muscles (quadriceps femoris), assessed at 3 weeks after triple injection. (**c**) Hematoxylin and eosin staining of the control (upper panel) and Mst-siRNA/ATCOL-treated quadriceps muscle (lower panel). Scale bar, 50 μm. (**d**) Comparison of muscle weight/body weight index between the Mst-siRNA/ATCOL and control-siRNA/ATCOL-treated mice (0.048 ± 0.002 versus 0.043 ± 0.001 $n=5$; $P<0.01$). (**e**) Distribution of myofibril sizes of the control and Mst-siRNA/ATCOL-treated quadriceps muscles. The right panel shows the average myofibril size (33.92 ± 2.91 versus 22.95 ± 1.54 μm, $n=156$; $P<0.01$).

mass was observed in the Mst-siRNA/ATCOL-treated muscle (Figure 2a). Western blot analysis showed that the protein levels of myostatin in the muscles treated with the Mst-siRNA/ATCOL complex were significantly decreased (average ratio 0.55 ± 0.03), but not in the contralateral muscles treated with control siRNAs/ATCOL complex (average ratio 0.83 ± 0.01) (Figure 2b; $P<0.05$, $n=5$). Furthermore, immunohistochemical analysis on the masseter using an anti-laminin α2 antibody showed increase in the mean myofiber size of the Mst-siRNA/ATCOL-treated muscle (Figure 2c), as is the case for the wild-type (not shown). On the basis of these results, it seems that myostatin maintains satellite cells or muscle stem cells in a quiescent state. Reduced myostatin activity would lead to activation of these cells and fusion into existing fibers (Supplementary Figure S1e and f), resulting in fiber hypertrophy as proposed previously.[14]

We further examined whether systemic administration of the Mst-siRNA/ATCOL complex would have an effect on silencing the myostatin expression and lead to muscle enlargement. The Mst- or control siRNA/ATCOL complex was applied intravenously into normal mice four times in 3 weeks. Strikingly, we observed an obvious enlargement of skeletal muscles of lower limbs (Figure 3a), masseters and other muscles. Since change in the muscles of lower limbs is much larger than others, we used them for further analyses. We confirmed reduction of myostatin proteins in the muscles treated with the Mst-siRNA/ATCOL complex (average ratio 0.67 ± 0.11) (Figure 3b; $P<0.01$, $n=5$; average ratio for control 0.87 ± 0.03). We observed that the treated lower limbs are much larger than the controls, although the average body weights were 26.7 ± 0.7 and 25.8 ± 0.4 g for controls and treated mice, respectively. No increase in the body weight of the treated mouse was observed, probably because increase in the muscle weight compensated for reduction of fat accumulation.[17] To show increase in muscle weights, we used the muscle weight/body weight ratio (Figure 3d), in case the body weight exhibited variation. Significant increase in muscle fiber size (Figures 3c and e) was also observed after 3 weeks. These results indicate that siRNAs targeting against myostatin, intravenously administered with ATCOL, can specifically repress the expression of myostatin, inducing muscle hypertrophy in normal mice.

We present evidence that local and systemic applications of siRNA against myostatin coupled with ATCOL markedly stimulate muscle growth *in vivo* within a few

weeks. Local application of siRNA/ATCOL complex was shown to be effective to target the vascular endothelial growth factor gene in a xenografted tumor,[18] while ATCOL was used for systemic siRNA delivery into tumor-bearing mouse models and proved to be effective for silencing exogenous genes as luciferase and metastasis-associated genes as EZH2.[6] However, it has not been elucidated until this study whether the siRNA complex could have an effect of muscle growth on normal tissues by repression of muscle-specific genes. It has been thought that the enhanced permeability and retention (EPR) effect in tumor tissues could facilitate selective targeting of siRNA/polymer complex.[6] In spite of the significance of the EPR effect in tumor therapies, it is noticeable that normal and nontumor diseased tissues can be targets for siRNA-based drugs applied systemically. It was reported that nuclease activity to siRNA could be prevented[18] and cellular uptake of siRNAs was elevated by ATCOL.[5] Although the precise mechanisms by which ATCOL achieves these effects have not been elucidated to date, ATCOL complexed with DNA molecules was demonstrated to be efficiently transduced into mammalian cells.[19] Thus, similarly siRNA/ATCOL complexes may be transduced into cells probably by the same mechanisms as observed for DNA molecules. As a simple administration of myostatin-siRNA/ATCOL complex has a muscle growth effect, this novel method for fighting against muscle atrophy would be of considerable value for clinical applications. In tumor-bearing mice, it was reported that ATCOL could distribute siRNAs against luciferase to normal liver, lung, spleen and kidney tissues as well as bone-metastatic lesions.[6] ATCOL was also reported to display low toxicity and low immunogenicity when it is transplanted *in vivo*.[20,21] Taken together with our results, application of siRNAs with ATCOL would be promising for a therapeutic remedy against various diseases not only of muscles, but also of these organs.

## Acknowledgements

We thank Drs Shin-ichiro Nishimatsu, Tsutomu Nohno, Department of Molecular Biology, Kawasaki Medical School for valuable advice. We also thank Shizuka Sasano, Division of Neurology, Kawasaki Medical School and Megumu Kita, Laboratory Animal Center, Kawasaki Medical School for their technical assistances. This work was supported by a Research Grant (14B-4) for Nervous and Mental Disorders from the Ministry of Health, Labour and Welfare; a Grant (15131301) for Research on Psychiatric and Neurological Diseases and Mental Health from the Ministry of Health, Labour and Welfare of Japan and from JSPS KAKENHI (14370212) to SN, YO and YS and by Research Project Grants (15-115B and 16-601) from Kawasaki Medical School to YO and YS.

## References

1 Fire A, Xu S, Montgomery MK, Kostas SA, Driver SE, Mello CC. Potent and specific genetic interference by double-stranded RNA in *Caenorhabditis elegans*. *Nature* 1998; **391**: 806–811.
2 Elbashir SM, Harborth J, Lendeckel W, Yalcin A, Weber K, Tuschl T. Duplexes of 21-nucleotide RNAs mediate RNA interference in cultured mammalian cells. *Nature* 2001; **411**: 494–498.
3 de Fougerolles A, Vornlocher HP, Maraganore J, Lieberman J. Interfering with disease: a progress report on siRNA-based therapeutics. *Nat Rev Drug Discov* 2007; **6**: 443–453.
4 Gary DJ, Puri N, Won YY. Polymer-based siRNA delivery: perspectives on the fundamental and phenomenological distinctions from polymer-based DNA delivery. *J Control Release* 2007; **121**: 64–73.
5 Minakuchi Y, Takeshita F, Kosaka N, Sasaki H, Yamamoto Y, Kouno M *et al*. Atelocollagen-mediated synthetic small interfering RNA delivery for effective gene silencing *in vitro* and *in vivo*. *Nucleic Acids Res* 2004; **32**: e109.
6 Takeshita F, Minakuchi Y, Nagahara S, Honma K, Sasaki H, Hirai K *et al*. Efficient delivery of small interfering RNA to bone-metastatic tumors by using atelocollagen *in vivo*. *Proc Natl Acad Sci USA* 2005; **102**: 12177–12182.
7 Takeshita F, Ochiya T. Therapeutic potential of RNA interference against cancer. *Cancer Sci* 2006; **97**: 689–696.
8 McPherron AC, Lawler AM, Lee SJ. Regulation of skeletal muscle mass in mice by a new TGF-beta superfamily member. *Nature* 1997; **387**: 83–90.
9 Deconinck N, Dan B. Pathophysiology of Duchenne muscular dystrophy: current hypotheses. *Pediatr Neurol* 2007; **36**: 1–7.
10 Foster K, Foster H, Dickson JG. Gene therapy progress and prospects: Duchenne muscular dystrophy. *Gene Therapy* 2006; **13**: 1677–1685.
11 Bogdanovich S, Krag TO, Barton ER, Morris LD, Whittemore LA, Ahima RS *et al*. Functional improvement of dystrophic muscle by myostatin blockade. *Nature* 2002; **420**: 418–421.
12 Nishi M, Yasue A, Nishimatsu S, Nohno T, Yamaoka T, Itakura M *et al*. A missense mutant myostatin causes hyperplasia without hypertrophy in the mouse muscle. *Biochem Biophys Res Commun* 2002; **293**: 247–251.
13 Ohsawa Y, Hagiwara H, Nakatani M, Yasue A, Moriyama K, Murakami T *et al*. Muscular atrophy of caveolin-3-deficient mice is rescued by myostatin inhibition. *J Clin Invest* 2006; **116**: 2924–2934.
14 Magee TR, Artaza JN, Ferrini MG, Vernet D, Zuniga FI, Cantini L *et al*. Myostatin short interfering hairpin RNA gene transfer increases skeletal muscle mass. *J Gene Med* 2006; **8**: 1171–1181.
15 Artaza JN, Bhasin S, Magee TR, Reisz-Porszasz S, Shen R, Groome NP *et al*. Myostatin inhibits myogenesis and promotes adipogenesis in C3H 10T(1/2) mesenchymal multipotent cells. *Endocrinology* 2005; **146**: 3547–3557.
16 Bulfield G, Siller WG, Wight PA, Moore KJ. X chromosome-linked muscular dystrophy (mdx) in the mouse. *Proc Natl Acad Sci USA* 1984; **81**: 1189–1192.
17 McPherron AC, Lee SJ. Suppression of body fat accumulation in myostatin-deficient mice. *J Clin Invest* 2002; **109**: 595–601.
18 Takei Y, Kadomatsu K, Yuzawa Y, Matsuo S, Muramatsu T. A small interfering RNA targeting vascular endothelial growth factor as cancer therapeutics. *Cancer Res* 2004; **64**: 3365–3370.
19 Honma K, Ochiya T, Nagahara S, Sano A, Yamamoto H, Hirai K *et al*. Atelocollagen-based gene transfer in cells allows high-throughput screening of gene functions. *Biochem Biophys Res Commun* 2001; **289**: 1075–1081.
20 Ochiya T, Nagahara S, Sano A, Itoh H, Terada M. Biomaterials for gene delivery: atelocollagen-mediated controlled release of molecular medicines. *Curr Gene Ther* 2001; **1**: 31–52.
21 Sano A, Maeda M, Nagahara S, Ochiya T, Honma K, Itoh H *et al*. Atelocollagen for protein and gene delivery. *Adv Drug Deliv Rev* 2003; **55**: 1651–1677.

Supplementary Information accompanies the paper on Gene Therapy website (http://www.nature.com/gt)

*Am J Physiol Endocrinol Metab* 300: E543–E553, 2011.
First published January 4, 2011; doi:10.1152/ajpendo.00430.2010.

# Follistatin-derived peptide expression in muscle decreases adipose tissue mass and prevents hepatic steatosis

**Masashi Nakatani,[1] Masahiro Kokubo,[2] Yutaka Ohsawa,[3] Yoshihide Sunada,[3] and Kunihiro Tsuchida[1]**

[1]*Division for Therapies against Intractable Diseases, Institute for Comprehensive Medical Science (ICMS), and* [2]*Joint Research Laboratories, Fujita Health University, Toyoake; and* [3]*Division of Neurology, Department of Internal Medicine, Kawasaki Medical School, Kurashiki, Japan*

Submitted 20 July 2010; accepted in final form 3 January 2011

**Nakatani M, Kokubo M, Ohsawa Y, Sunada Y, Tsuchida K.** Follistatin-derived peptide expression in muscle decreases adipose tissue mass and prevents hepatic steatosis. *Am J Physiol Endocrinol Metab* 300: E543–E553, 2011. First published January 4, 2011; doi:10.1152/ajpendo.00430.2010.—Myostatin, a member of the transforming growth factor (TGF)-β superfamily, plays a potent inhibitory role in regulating skeletal muscle mass. Inhibition of myostatin by gene disruption, transgenic (Tg) expression of myostatin propeptide, or injection of propeptide or myostatin antibodies causes a widespread increase in skeletal muscle mass. Several peptides, in addition to myostatin propeptide and myostatin antibodies, can bind directly to and neutralize the activity of myostatin. These include follistatin and follistatin-related gene. Overexpression of follistatin or follistatin-related gene in mice increased the muscle mass as in myostatin knockout mice. Follistatin binds to myostatin but also binds to and inhibits other members of the TGF-β superfamily, notably activins. Therefore, follistatin regulates both myostatin and activins in vivo. We previously reported the development and characterization of several follistatin-derived peptides, including FS I-I (Nakatani M, Takehara Y, Sugino H, Matsumoto M, Hashimoto O, Hasegawa Y, Murakami T, Uezumi A, Takeda S, Noji S, Sunada Y, Tsuchida K. *FASEB J* 22: 477–487, 2008). FS I-I retained myostatin-inhibitory activity without affecting the bioactivity of activins. Here, we found that inhibition of myostatin increases skeletal muscle mass and decreases fat accumulation in FS I-I Tg mice. FS I-I Tg mice also showed decreased fat accumulation even on a control diet. Interestingly, the adipocytes in FS I-I Tg mice were much smaller than those of wild-type mice. Furthermore, FS I-I Tg mice were resistant to high-fat diet-induced obesity and hepatic steatosis and had lower hepatic fatty acid levels and altered fatty acid composition compared with control mice. FS I-I Tg mice have improved glucose tolerance when placed on a high-fat diet. These data indicate that inhibiting myostatin with a follistatin-derived peptide provides a novel therapeutic option to decrease adipocyte size, prevent obesity and hepatic steatosis, and improve glucose tolerance.

myostatin; adipocyte; fatty liver; glucose tolerance

THE TRANSFORMING GROWTH FACTOR (TGF)-β superfamily is one of the largest families of secreted growth and differentiation factors and plays important roles in regulating tissue development and homeostasis (37). Myostatin, a member of the TGF-β superfamily, acts as a negative regulator of muscle growth (19, 22). Mutations in the myostatin gene in cattle, sheep, dogs, and humans cause an increase in skeletal muscle mass, indicating conservation of its function in mammals (5, 8, 23, 26, 32, 33). Myostatin is expressed predominantly in skeletal muscle and at significantly lower levels in adipose tissue (22). Inhibition of myostatin causes an increase in skeletal muscle mass and ameliorates several models of muscular dystrophies. Therefore, myostatin inhibitors are a promising therapeutic target to treat muscular atrophy and muscular dystrophy (19, 29, 37).

The loss of myostatin by gene disruption prevents an age-related increase in adipose tissue mass and partially attenuates the obese and diabetic phenotypes (14, 24). The serum leptin concentration and adipose tissue leptin mRNA expression were lower in myostatin null mice than in wild-type mice (24). Inhibition of myostatin by transgenic (Tg) expression of myostatin propeptide was also reported to prevent diet-induced obesity (41, 42). Even when fed a high-fat diet (HFD), these mice exhibited normal insulin sensitivity, unlike wild-type mice (42). Furthermore, ΔACVR2B, a soluble extracellular form of the activin type IIB receptor, effectively decreased the adipose tissue mass (1). These results suggest that inhibition of myostatin signaling could be useful to prevent and/or treat obesity and diabetes.

There are several strategies to block the functions of myostatin, including myostatin propeptide, follistatin, follistatin-related gene (FLRG), follistatin domain-containing growth and differentiation factor-associated serum protein-1 (GASP-1), the potent myostatin inhibitor ΔACVR2B, neutralizing antibodies, and small chemical compounds that block receptor serine kinases (2, 15, 37, 38).

Follistatin was shown to bind to myostatin and inhibit its activity. However, follistatin inhibits other members of the TGF-β superfamily, including GDF11 and activin (11, 37, 38). Although GDF11 and myostatin show a high degree of sequence similarity at the amino acid level, GDF11 is unlikely to regulate skeletal muscle mass, because GDF11 controls skeleton and kidney development rather than regulating muscle mass (21). Like myostatin, activin regulates skeletal muscle mass (12). However, unlike myostatin, activin has many pleiotropic roles including ovarian and neuronal functions (30, 36). In our previous study, we reported the development and characterization of a myostatin inhibitor derived from follistatin, designated FS I-I. FS I-I is unable to neutralize activin but still binds to and inhibits myostatin (27). Tg expression of FS I-I using a skeletal muscle-specific promoter caused a widespread increase in skeletal muscle mass and ameliorated muscular dystrophy. In addition, muscle strength was recovered when the FS I-I Tg mice were crossed with *mdx* mice (27). In this study, we explored whether FS I-I Tg mice are resistant to diet-induced obesity and hepatic steatosis. We found that FS I-I Tg mice exhibited reduced fat accumulation even when fed a normal diet (NFD). Adipocytes were also much smaller than those of wild-type littermates. Furthermore, the FS I-I Tg mice

Address for reprint requests and other correspondence: K. Tsuchida, Division for Therapies against Intractable Diseases, Institute for Comprehensive Medical Science (ICMS), Fujita Health Univ., Toyoake, Aichi 470-1192, Japan (e-mail: tsuchida@fujita-hu.ac.jp).

were resistant to HFD-induced obesity and hepatic steatosis. The liver of HFD-fed FS I-I Tg mice showed significantly different fatty acid composition compared with that seen in the control mice. Our studies suggest that follistatin-derived myostatin inhibitors offer a therapeutic option for obesity, diabetes, and hepatic steatosis.

## MATERIALS AND METHODS

*Animals.* The establishment of skeletal muscle-specific FS I-I Tg mice is described in our previous paper (27). In brief, *Eco*RI-*Sma*I fragment covering the whole coding sequence of FS I-I was subcloned into the MDAF2 vector containing the myosin light-chain promoter SV40 processing sites and MLC1/3 enhancer. *Cla*I fragment with 3.9 kb was microinjected to produce FS I-I transgenic mice (27). The transgene was expressed in skeletal muscles but not in cardiac muscle or adipose tissues. FS I-I Tg male mice and wild-type littermates were obtained from the offspring of FS I-I Tg mice mated with C57BL/6 mice. The genotypes were determined by PCR as previously described (27). The FS I-I Tg and littermate male mice were weaned at 4 wk of age and given free access to either a normal-fat (NFD; 5% kcal fat; CE-2; CLEA, Shizuoka, Japan) or a high-fat diet (HFD; 32% kcal fat, High Fat Diet 32, CLEA) from 4 to 13 wk. Food intake did not differ between the two genotypes on the HFD. Body weight was recorded every week. All mice were housed in cages with a constant temperature (22°C) and a 12:12-h light-dark cycle. All experiments were performed at the Laboratory Animal Center with approval from the Animal Research Committee at Fujita Health University.

*Analysis of adipose tissue, skeletal muscle, and liver.* Adipose tissues (retroperitoneal, epididymal, and inguinal fat pads), skeletal muscles [tibialis anterior (TA), extensor digitorum longus (EDL), quadriceps femoris (Qf), and soleus], and liver samples were obtained from mice at 13 or 20 wk of age. Adipose tissue and muscles were also obtained from NFD- and HFD-fed mice at *week 13*. The wet tissue weights were measured.

*Histological analyses of adipose tissues and liver.* The adipose tissues and livers either from FS I-I Tg mice or littermates were fixed in 4% paraformaldehyde (PFA), dehydrated in ethanol, embedded in paraffin, and sectioned at a thickness of 6 μm. The sections were then deparaffinized, rehydrated, and stained with hematoxylin and eosin (H&E). The area of adipocytes was determined in images stained with H&E. The area of 200 adipocytes per mouse was determined in five wild-type and five FSI-I Tg mice (1,000 adipocytes for each genotype), and the average cell area was determined. Morphometric analyses to measure adipocyte area and size were performed using WinROOF software (Mitani, Fukui, Japan).

*Electron microscope analysis.* Adipose tissue samples were fixed for 4 h with 2% PFA and 2.5% glutaraldehyde in phosphate-buffered saline (PBS) at room temperature. The specimens were then postfixed at room temperature for 1 h with 2% osmium tetroxide in Millonig's buffer containing 0.54% glucose and dehydrated through an ethanol gradient. For scanning electron microscopy, the dehydrated specimens were then immersed in *t*-butyl alcohol, dried using a freeze-drying device, coated with gold using an ion sputtering device (JEE-420T, JEOL), and examined under a scanning electron microscope (H7650; Hitachi, Tokyo, Japan). For transmission electron microscopy, specimens were immersed in QY-1 (Nisshin EM, Tokyo, Japan), embedded in epoxy resin (Epon812; Polyscience, Wako Pure Chemical Industries, Osaka, Japan), and cut into ultrathin sections. The sections were stained with uranyl acetate and lead citrate, followed by transmission electron microscopy at an accelerating voltage of 80 kV (JEM-1010TEM, JEOL). One hundred fifty mitochondria of epididymal adpipocytes each from three wild-type and FS I-I Tg mice were analyzed using WinROOF software.

*Quantitative real-time PCR.* The relative expressions of uncoupling protein-3 (UCP3), acetyl-CoA carboxylase-1 (ACC1), stearoyl-CoA desaturase-1 (SCD1), glucokinase (Gck), and phosphofructokinase (PFK) were determined by quantitative (q)PCR using a TAKARA Thermal Cycler Dice Real-Time System (Takara Bio, Shiga, Japan). Briefly, mRNA was isolated from liver and adipose tissues from FS I-I Tg mice and wild-type littermates by use of TRIzol (Invitrogen, Tokyo, Japan) with standard techniques. The isolated RNA was cleaned by DNaseI and purified using RNeasy Tissue kits (Qiagen, Tokyo, Japan). Reverse transcription was carried out with 500 ng of RNA using QuantiTect reverse transcription kits (Qiagen) according to the manufacturer's instructions.

We used Primer 3 software to design the primers for UCP3 (forward: 5′-CCGGTGGATGTGGTAAAGAC-3, reverse: 5′-AAGCTCCCAGACGCAGAAAG-3); ACC1 (forward: 5′-CCCATCCAAACAGAGGGAAC-3, reverse: 5-CTGACAAGGTGGCGTGAAG-3); SCD1 (forward: 5′-CAAGCTGGAGTACGTCTGGA-3′, reverse: 5′-CAGAGCGCTGGTCATGTAGT-3′); Gck (forward: 5′-TGGGCTTCACCTTCTCCTTC-3′, reverse: 5′-CGATGTTGTTCCCTTCTGCT-3′); and PFK (forward: 5′-GAAGCCAATCACCTCAGAAGAC-3′, reverse: 5′-TTCCACACCCATCCTGCT-3′). Each well of the 96-well reaction plate contained a total volume of 25 μl. cDNA (0.5 μl) solution was combined with each of forward and reverse primers (10 μM), distilled water, and SYBR Premix Ex Taq (Takara Bio). All reactions were performed in triplicate. The relative amounts of RNAs were calculated using the comparative $C_T$ method. We used hepatic glyceraldehyde-3-phosphate dehydrogenase (GAPDH) and adipose tissue 36B4 as controls. Significant differences between the wild-type and FS I-I Tg mice were analyzed by Student's *t*-test.

*Western blotting.* Adipose tissues (epididymal and inguinal fat pads), skeletal muscle (Qf), and liver were dissected from wild-type and FSI-I Tg mice. Samples were homogenized in a buffer containing 50 mM Tris·HCl, pH 7.5, 150 mM NaCl, 5 mM NaF, 1% Nonidet P-40, 5 mM β-glycerophosphate, 1 mM phenylmethylsulfonyl fluoride, 4 μg/ml leupeptin, and 1 μg/ml aprotinin and centrifuged at 15,000 rpm for 10 min at 4°C, and the lipid-free lysates were collected. Aliquots of the lysates containing 30 μg of protein or serum containing 60 μg of protein were separated by sodium dodecyl sulfate-polyacrylamide gel electrophoresis and transferred onto polyvinylidene difluoride membranes. The membrane was blocked in 5% skim milk for 1 h at room temperature. The membranes were then probed with anti-cytochrome *c*, phosphorylated Smad 3, or Smad 3 (Cell Signaling Technology, Beverly, MA) at 4°C overnight (1:1,000 dilution), followed by incubation with horseradish peroxidase-conjugated secondary antibodies and chemiluminescence reactions by ECL plus (GE Healthcare, Tokyo, Japan). As a loading control, antibodies to tubulin or actin (Cell Signaling Technology, Beverly, MA) were used. Detection of FS I-I or follistatin by Western blotting was performed using rabbit polyclonal antibodies (ABPIII) raised against follistatin domain I of follistatin (31). Images of the developed immunoblots were captured using a cooled CCD camera system (Light-Capture; ATTO, Tokyo, Japan).

*Measurement of serum parameters and triglycerides.* Wild-type and FS I-I Tg mice ($n$ = 4–6 per group) fed the NFD or HFD from *weeks 4* to *13* of age were fasted overnight at *week 13* for 16 h before blood sampling. The triglyceride, nonesterified fatty acid (NEFA), cholesterol, fasting glucose, insulin, leptin, and adiponectin concentrations were measured in serum samples prepared from whole blood collected from the retroorbital venous plexus of anesthetized mice. Plasma, total cholesterol, and NEFA were measured using enzymatic assays (triglyceride E, cholesterol E, and NEFA tests, respectively; Wako Pure Chemical Industries, Osaka, Japan). Plasma leptin, adiponectin, and insulin levels were measured using enzyme-linked immunoassays from Morinaga (Kanagawa, Japan), R&D systems (Gunma, Japan), and Otsuka (Tokyo, Japan), respectively. Triglycerides from liver and skeletal muscle were extracted with chloroform-methanol (2:1, vol/vol), centrifuged twice to remove debris, dried, and resuspended in 2-propanol containing 10% Triton X-100 (17). Triglyceride contents were enzymatically measured using a triglyceride E test. Mouse preadipocyte 3T3-L1 cells and human hepatocyte Hep

G2 cells were grown in Dulbecco's modified Eagle's medium (DMEM) supplemented with 10% fetal calf serum. Cells ($1 \times 10^5$)/12-well plates of differentiating 3T3-L1 cells were stimulated with either 80 ng/ml FS I-I or 40 ng/ml myostatin (R&D systems) for 3 days. Hep G2 cells treated with 3 mg/ml glucose, 10 μg/ml insulin, and either 80 ng/ml FS I-I or 40 ng/ml myostatin for 3 days. Cellular triglycerides were extracted and measured as described above. All assays were performed according to the manufacturer's protocol.

*Glucose tolerance test.* Glucose tolerance tests were performed in six to eight mice per group at 13 wk of age after being fed the NFD or HFD for 9 wk. The mice were fasted overnight and then received an intraperitoneal injection of 10% dextrose (1 g/kg body wt). Blood was collected from the tail at 0, 15, 30, 60, and 120 min after dextrose injection, and blood glucose was measured using an Accu-Check glucose monitor (Roche Diagnostic, Indianapolis, IN).

*Insulin tolerance test.* Insulin tolerance tests were performed in five mice per group at 13 wk of age after being fed the HFD for 9 wk. The mice were starved for 16 h and received an intraperitoneal injection of human insulin (0.75 U/kg body wt; Sigma-Aldrich Japan). Blood glucose was measured at 0, 30, 60, and 90 min after injection using an Accu-Check glucose monitor (24).

*Measurement of hepatic fatty acid content.* Approximately 100 mg of liver tissue was obtained from wild-type and FS I-I Tg mice fed the NFD or HFD for 9 wk ($n = 6$ per group). Lipids were extracted using the Bligh-Dyer chloroform-methanol method (4). The extracted lipids were dissolved in 1 ml of chloroform and subjected to methanolysis-gas chromatographic analysis (3). Methyl stearate was used to generate a standard curve for quantitation. The determinations were repeated at least twice, and essentially the same results were obtained.

*Metabolic rate analysis.* Oxygen consumption was measured with an indirect calorimetric metabolism measuring system (model MK-5000RQ, Muromachikikai) (17). Each mouse was kept in a sealed chamber with an air flow of 0.6 l/min for 2 h during the light cycle. Air was sampled every 3 min, and the consumed oxygen concentration ($\dot{V}O_2$) was calculated (24). Five mice each for wild-type and FS I-I Tg mice fed NMD were analyzed.

*Statistical analysis.* Results are presented as means ± SD. Statistical significance was assessed by Student's *t*-tests. Differences between groups were considered statistically significant at $P < 0.05$. *P* values are presented in figure and table legends.

## RESULTS

*Decreased fat accumulation in FS I-I tg mice.* We previously reported (27) that FS I-I Tg mice show a marked increase in skeletal muscle mass compared with wild-type mice when fed a NFD. Intriguingly, even with a NFD, FS I-I Tg mice showed age-dependent decreased fat accumulation. Although there was no difference in individual fat pad weights between wild-type and FS I-I Tg mice at 13 wk of age (data not shown), there was a significant difference at 20 wk of age. For example, at 20 wk of age, the weight of the epididymal fat pad was 60% lower in FS I-I Tg mice than in wild-type mice (Fig. 1*A*). Furthermore, the weights of the inguinal and retroperitoneal fat pads of FS I-I Tg mice were 33 and 67% lower, respectively, in FS I-I Tg mice than in wild-type mice. Therefore, we quantified the adipocyte size histologically using H&E staining (Fig. 1*B*)

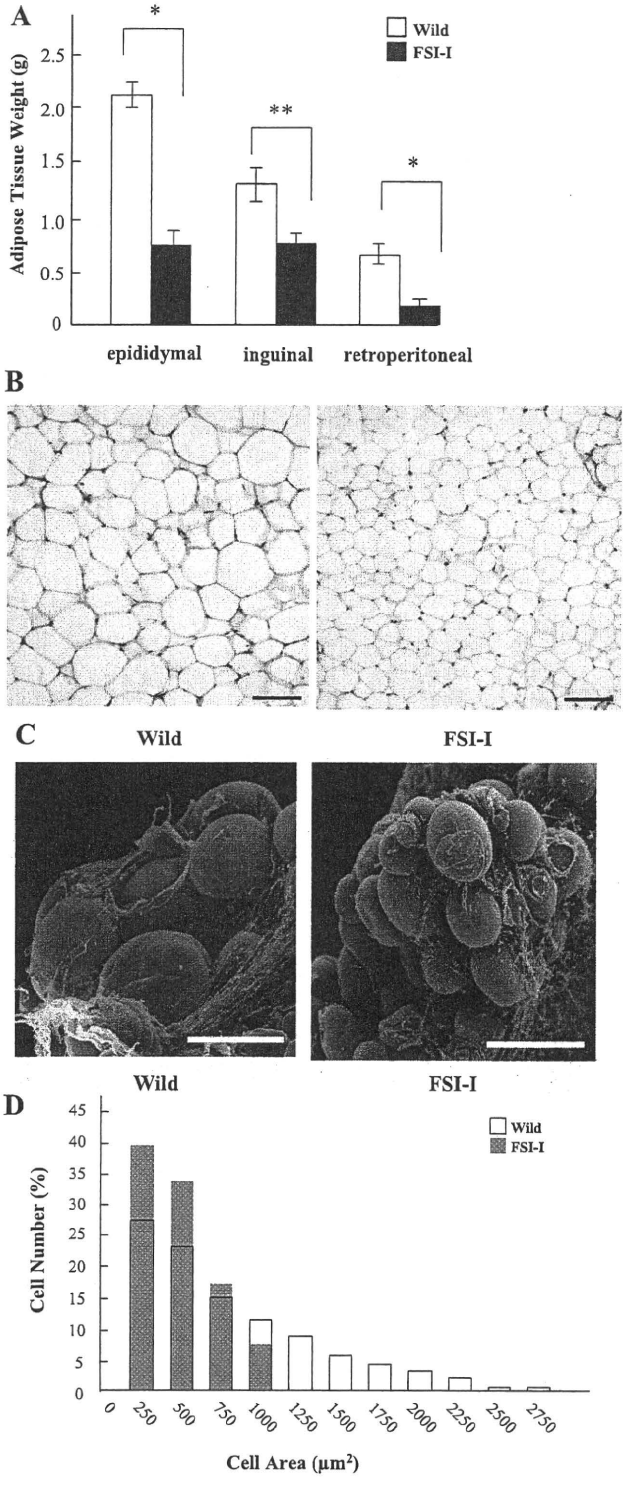


Fig. 1. *A*: adipose tissue weights (g) of 20-wk-old male wild-type and transgenic (Tg) mice with a myostatin inhibitor derived from follistatin [follistatin (FS)-derived peptide (FS I-I)] fed a control diet. Epididymal, inguinal, and retroperitoneal fat pads from 5 mice each from wild-type and FSI-I Tg mice were dissected and weighed. $^*P < 0.005$ and $^{**}P < 0.03$, Student's *t*-test. *B*: histological analysis of adipose tissues. Epididymal fat pads from 20-wk-old wild-type and FS I-I Tg mice were sectioned and stained with H&E. Scale bar, 100 μm. *C*: scanning electron microscopy of epididymal fat pads. 20-wk-old wild-type (*left*) and FS I-I Tg mice (*right*) were analyzed. Scale bar, 120 μm. *D*: distribution of epididymal adipocyte area in 20-wk-old wild-type and FS I-I Tg mice; 200 adipocytes were counted per mouse (5 mice per group). The percentage of adipocytes with indicated areas per total adipocytes was calculated and plotted. The mean adipocyte area was smaller in FS I-I Tg mice (717.4 ± 579.1 μm²) than in wild-type mice (436.8 ± 309.1 μm²).

and by scanning electron microscopy (Fig. 1*C*). Both techniques confirmed that adipocyte size was smaller in FS I-I Tg mice than in wild-type mice. Therefore, we determined the mean adipocyte area. Quantification of the area of individual adipocytes is shown in Fig. 1*D*. At *week 20* of age, the mean adipocyte area was smaller in FS I-I Tg mice than in wild-type mice (436.8 ± 309.1 vs. 717.4 ± 579.1 $\mu m^2$, respectively; Fig. 1*D*). These results indicate that FS